Numerical design and test on an assembled structure of a bolted joint with viscoelastic damping

Chaima HAMMAMI [1], Etienne BALMES [1,2], Mikhail GUSKOV [1]

[1] : Arts et Métiers Paritech, PIMM, 151 boulevard de l'hôpital, 75013 Paris, France

[2] : SDTools, 44 Rue Vergniaud, 75013 Paris, France

Abstract: Mechanical assemblies are subjected to many dynamic loads and modifications are often needed to achieve acceptable vibration levels. While modifications on mass and stiffness are well mastered, damping modifications are still considered difficult to design. The paper presents a case study on the design of a bolted connection containing a viscoelastic damping layer. The notion of junction coupling level is introduced to ensure that sufficient energy is present in the joints to allow damping. Static performance is then addressed and it is shown that localization of metallic contact can be used to meet objectives, while allowing the presence of viscoelastic materials. Numerical prediction of damping then illustrates difficulties in optimizing for robustness. Modal test results of three configurations of an assembled structure, inspired by aeronautic fuselages, are then compared to analyze the performance of the design. While validity of the approach is confirmed, the effect of geometric imperfections is shown and stresses the need for robust design.

Keywords: damping, design, bolted joints, coupling, viscoelastic material, experiments.

1. Introduction

Vibrations in mechanical assemblies often cause damage, noise and discomfort. The introduction of additional dissipation limits vibration levels and can thus significantly improve performance. This work will focus on the damping generated by joints incorporated in a structure typical of aeronautic construction. Since materials used in these structures are typically lightly damped, junctions clearly appear as areas where additional damping can be introduced. Nevertheless, a trade-off between the relative motion of the connected surfaces enabling for dissipation and the stiffness of the junction is to be found. The main physical dissipation mechanisms found in junctions are contact / friction, e.g. [1]–[3], and viscoelastic behavior of materials, such as [4]–[6].

Vibration damping has been the object of many studies [7]–[10]. However, treating damping design in assemblies has, in the last decade, been a significant interest for the aerospace and automotive sectors as illustrated in [11]–[13]. The treatment of the whole structures, as in [4] or [14], has not been the object of much literature. The most common joint geometries are flat lap joints with bolts, rivets or weld spots working in shear, and bracketed joints with folded plates and connectors working in traction [7]. The present paper will illustrate a design process for the latter.

The work is focused on the viscoelastic behavior of materials and illustrates how a numerical approach can be used to guide the design of dissipative assemblies. Taking a global dynamics of two fuselage segments, the objective is to redesign the joints to maximize dissipation while preserving the base function of a bolted junction. More specifically, this work presents a new approach to use the dissipative effect of viscoelastic materials, while preserving the functional state of junctions. The first

notion introduced is a level of coupling, which measures the influence of a junction on the overall dynamics and is strongly correlated with the ability of the junctions to dissipate.

The study is carried out on a testbed shown in Figure 1. The structure is typical of aeronautic fuselage construction with frames and longerons providing a base structure and skins enclosing the whole. The testbed objective being to focus on the damping added by junctions between fuselage segments, one considers a main component "big box" connected to a "small box" that is clamped to the ground. This design limits the testbed size while generating significant loads in the connection between the two parts. Each box is welded to minimize internal damping and ensure that the overall damping will be mostly due to the junction shown in Figure 1.

The configuration considered here uses bolted brackets with a web (thin plate) for additional stiffness. The brackets are riveted and glued to the skin in order to minimize dissipation sources. Partial tests have shown that dissipation induced by riveted and glued parts is extremely low and can be neglected for the rest of the work.

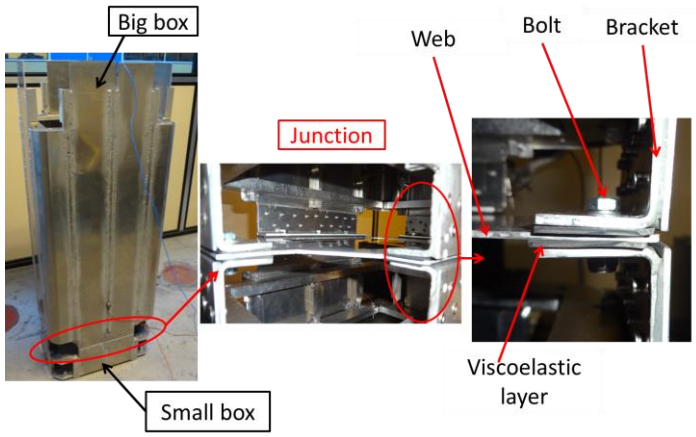

Figure 1 : Fuselage testbed *1155×409×259mm*

This paper is divided into two parts. The first part is about the finite element analysis done with bolted junctions incorporating viscoelastic materials. The coupling level in the junction is first investigated in section 2 since dissipation is its direct issue. Once this criterion is highlighted, a suggestion of a new design for dissipative bolted joints is detailed in section 3. The approach is based on reaching a compromise between the dissipative effect of viscoelastic materials and the functional static state of bolted joints. The addition of viscoelastic material can certainly increase the dissipation, while optimization is always desirable. Therefore, optimization strategies are then proposed in section 4. In the second part, an experimental investigation for normal modes is described and results are compared to numerical ones after identification process in section 5.1. Actually, mechanical structures have shape defects of variable importance due to machining or mounting processes. The impact of these defects on the damping design is thus discussed in section 5.2.

2. Coupling: a measure of joint influence

When designing a damping treatment, the first step is to evaluate the amount of energy present in the structural elements under consideration. This is similar to the notion of electromechanical coupling in designing active systems so that the term **joint coupling level** will be used here. This is easily seen in the well-known formulation of the modal strain energy method [15] where the global loss factor η_s in a structure is approximated by a strain energy weighted loss in various components

$$\eta_s = \sum \eta_c E_c \Big/ \sum E_c \tag{1}$$

with E_c the strain energy associated to component c of the structure and η_c the loss factor associated with its material. The energy fraction in the junction is thus a clear indication of how much damping can be obtained. As a result, when designing a junction, damped computations are actually not needed and computing the energy fractions with elastic modes is sufficient as will be illustrated here. Since partial sums of energies are not readily available in all software packages, it is worth noting that computing the shift of elastic mode frequency due to a change in stiffness of a junction is a simple strategy that gives the same information. This notion of frequency shift is used to estimate electromechanical coupling in active systems [16] .

To illustrate the concept of coupling level, one introduces a layer of material with variable modulus between the two brackets. This is called viscoelastic layer in Figure 2 where the FEM model of the full structure is also shown. Frames, longerons and the viscoelastic layer are modelled with volumes while skins, brackets and web are modelled with shell elements connected to the volumes by rigid link to account for median planes. The ten bolts are represented by beams with connections of the head to adjacent shells done with RBE3 elements. The testbed overall size is *1155×409×259mm*^{3}. It is made of aluminum (Young modulus $E = 72GPa$, Poisson ratio *v=0.3*, density ρ*=2700 kg/m*^{3}) and weighs about *20Kg*. To allow reproduction of analyzes, a FEM model of the testbed is provided in the common NASTRAN format as supplemental material.

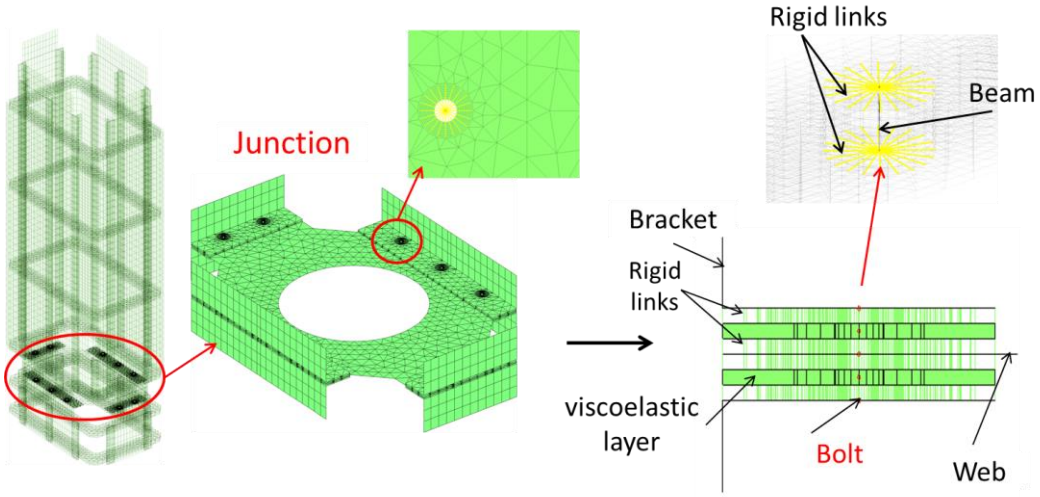

Figure 2 : Testbed model (42615 nodes, 46924 elements mixing shells, volumes and rigid links).

Figure 3a illustrates the coupling level by showing the strain energy fractions (Ek) of the viscoelastic layers, the ten bolts and the rest of the model as a function of the Young's modulus of the viscoelastic material. The strain energy of the viscoelastic material shows an important variation. In the shown range, the energy fraction in the viscoelastic layer shows an optimal value for $E_v = 3 \cdot 10^3 MPa$ where the energy fraction is close to 20%. For higher modulus the layer comes closer to perfect bonding and the energy fraction it contains decreases. For lower values of stiffness the coupling also decreases because the bond is too soft.

For very low values the strain is actually transferred to the bolts, for $E_v < 30MPa$, $Ek < 4\%$ in the viscoelastic layer, whereas for normal operation ($E_v > 10^3 MPa$,) the energy fraction in bolts is very

low ($Ek < 0.1\%$). The local deformation in the brackets, shown for the first bending mode in Figure 3b-c, confirms this trend as the viscoelastic material is compressed for $E_v = 72KPa$ thus inducing bolt bending, whereas nearly equal motion of all layers is found for $E_v = 100GPa$. This illustrates that the role of bolts is to maintain a contact surface, while the stiffness is provided by contacting surfaces rather than the bolt itself. Preserving this behavior will thus be considered as an important design feature that will be addressed in the next section.

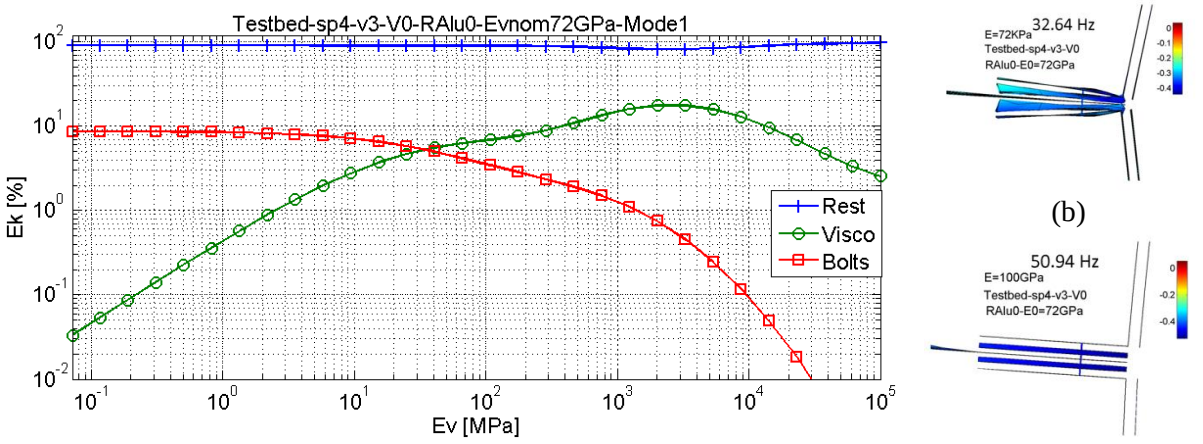

Figure 3 : a) Evolution of the strain energy fractions in the testbed model as function of the Young's modulus of the viscoelastic layer, b) first bending mode shape for $E_v = 72\ KPa$, c) first bending mode shape for $E_v = 100\ GPa$

As shown on Figure 3b-c, significant coupling is indeed associated with a strong frequency variation from 32 to $51Hz$ for the first bending mode. The first step of the proposed damping design procedure, proving that coupling level is sufficient, is thus accomplished here and following sections will demonstrate that significant damping can indeed be achieved.

3. Contact surface and joint stiffness

As shown in the previous section, the stiffness of a bolted junction is directly related to the contact area and the strain energy in the bolts associated with concerned modes is minimal. The main function of a bolt is thus to create an area of static preload to ensure a cohesive block behavior. While the end objective of this design study is to optimize damping, preserving static junction objectives is assumed to be critical and one will here seek to preserve the contact area in a junction, so that no global slip occurs and minimal dynamic stress is passed to the bolts thus avoiding potential fatigue problems.

To estimate the contact area, the first difficulty is to evaluate the load applied on the bolt. In fact, the exact value of this load is difficult to compute because of friction effects. The formula of Kellermann and Klein [17] is used here, giving the bolt pretension force $F = C/(\frac{p}{2\pi} + 0.583\mu_f + \frac{D}{2\mu_t})$, with C the clamping torque applied to the bolt, p the thread pitch, μ_f and μ_t the friction coefficients between threads and under the bolt head and D is the diameter under the bolt head/nut. This force is applied inside the shaft of the bolt. A compression area appears under the bolt head/nut which corresponds to the static contact area between components. A residual torque is typically found due to bolt torsion which can represent up to 40% of the clamping torque. [17] estimates its value by $C_t = F \cdot (\frac{p}{2\pi} + 0.583\mu_f)$.

The proper evaluation of the **preloaded surface** is a second question. From a computational point of view multiple bolt head models can be considered [18], [19]. The lap-joint model shown in Figure 4a uses volume elements to represent all bolt components, which is considered as the most realistic.

To study the loaded surface, Figure 4b shows the iso-values of the normal stress σ_{zz} within the plate as function of height and distance from the hole. The figure is generated for plates of thickness $h/2 = 4.7mm$, bolt head radius $R_{head} = 6.5mm$, hole radius $R_{hole} = 3.5mm$ and hexa20 solid elements. As expected, a large stress concentration is found at the hole edge. Away from this zone, the stress decreases gradually forming a cone-shaped distribution. Figure 4c displays normal stresses σ_{zi} at the plate interfaces as arrows. The maximum value is near the hole and a conical distribution continuously decreasing away from the hole is observed. The contact area can be defined by the area with sufficient contact pressure and corresponds to the intersection of the pressure cone with the contact surface.

Stiffness calculation theories [20] provide a surface estimate to build an equivalent bolt assembly stiffness. Here using Rasmussen's expression, the equivalent radius is $7.1mm$ (1.1 ·Rhead). This value corresponds to a radius with pressures close to $15\ MPa$ in Figure 4a-b and is thus underestimating the contact area. Other computations in [21] have shown that simplified bolt models constraints at the end of the beam give similar estimation of the area with sufficient static pressure to avoid macroscopic slip.

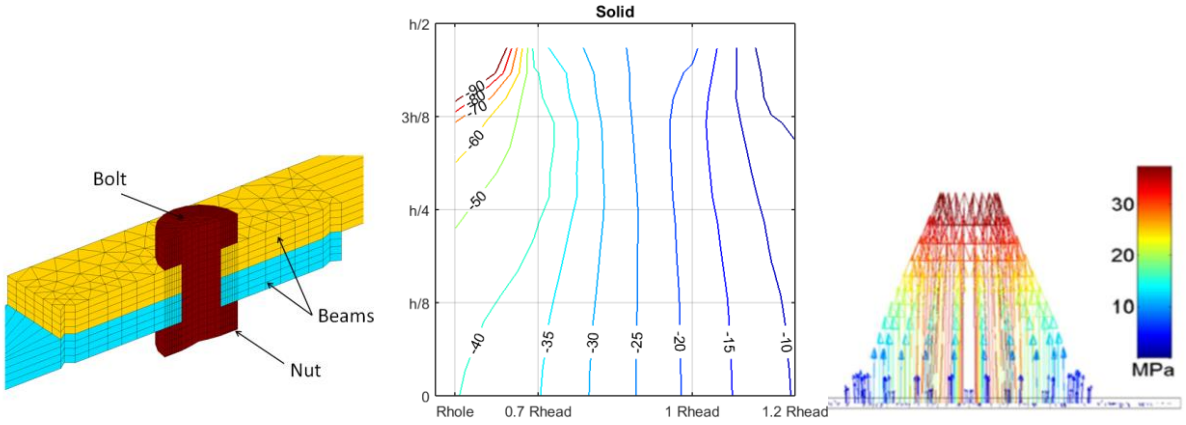

(a) (b) (c)

Figure 4 : (a) lap-joint model (b) Iso-values of σ_{zz} for solid model, (c) Normal stress at beam contacts testbed model with metallic contact interface

As a complement, a simulation with both preload force and residual torque was performed. It was found that shear stress induced by the residual torque where close to $1MPa$ and could be neglected considering the normal stresses of $45MPa$.

Considering that permanent contact is actually only guaranteed within the pressure cone existing under the bolt head, the proposition made here is to introduce a metallic part (washer) between components in contact under the bolted joint and to fill out the rest of the space with the viscoelastic material (Figure 5a-c). The metallic washer is used to preserve the non-slipping contact area, while the viscoelastic layer will provide damping.

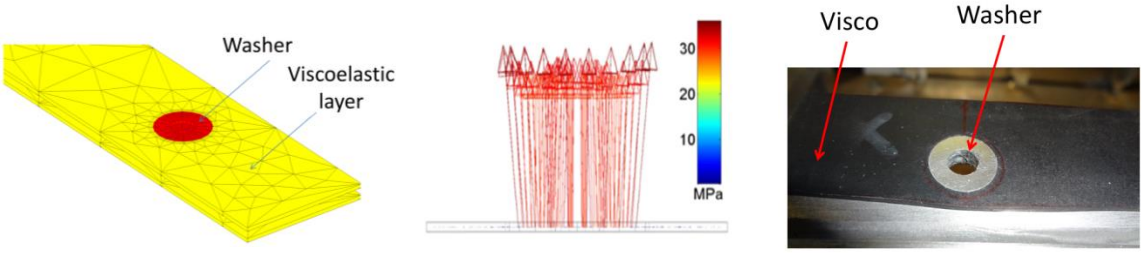

(a) (b) (c)

Figure 5 : a) Structuring of the contact interface in metallic and viscoelastic parts meshed using volume elements and connected to brackets using rigid links, b) Normal stresses at the testbed model with new contact interface, c) Implementation of the washer and the viscoelastic material in the testbed

To study static behavior of this new design, normal stresses induced by bolt preload are calculated at the bracket interface. The Young's modulus of the viscoelastic layer is taken to be $E_v = 70MPa$. Figure 5b displays the normal stresses distribution. Maximum values are very similar to that of metallic contact (Figure 4d) confirming preservation of the main characteristics. The distribution is however much more flat, with a jump to low values at the interface with the much softer viscoelastic material (between red arrows and blue ones which are small enough to look like points in Figure 5b). Non slipping contact is thus expected to be found for the same range of loads as metallic contact. With the proposed damping configuration, modeling bolts in the junction is no longer necessary since the preload ensures perfect metallic contact in the washer area.

4. Numerical optimization of viscoelastic properties

The proposed structuring of the contact surface into a washer, preserving stiffness below the bolt heads and thus the structural behavior of the bolts, and a viscoelastic layer, leaves open the question of optimizing the damping performance. One, thus, needs to define the thickness and material properties that will be needed to maximize damping.

In the frequency domain, the general form of forced response is

$$[Z(s)]\{q(s)\} = [Ms^2 + K(s)]\{q(s)\} = [b]\{u(s)\} \tag{2}$$

$$\{y(s)\} = [c]\{q(s)\} \tag{3}$$

where q is the degree of freedom vector, the load is the product of the input shape matrix b and the input u(s), Z is the matrix of dynamic stiffness resulting from combination of mass M and frequency dependent complex stiffness K. For linear viscoelastic materials dependence on history and temperature can in the frequency domain be represented as a complex modulus $E(s,T)$ which depends on frequency and temperature. This representation is independent of the choice of analytical or numeric representation for which many choices exist [22]. When assembling a model, one can group elements affected by a given modulus and rewrite the dynamic stiffness as a linear combination of fixed matrices with frequency dependent coefficients

$$K(s) = [K_e] + E(s)\left[\frac{K_v(E_0)}{E_0}\right] \tag{4}$$

where K_e and K_v are the stiffness matrix respectively of elastic and viscoelastic materials, E_0 is a reference elastic modulus, $E(s)$ is the complex frequency dependent modulus of the viscoelastic material.

For parametric studies, a multi-model reduction method [6], [23] is used in this work to reduce the problem size. A reduced dynamic stiffness can thus be written as

$$[Z(E(s),s)] = [s^2 T^t M T + T^t K_e T + E(s) T^t K_v(E_0) T] \tag{5}$$

where T is the orthonormalised reduction matrix defined as follows:

$$[T] = [\ldots \quad \Phi_{1:N}(E_\mathrm{i}) \quad \ldots] \tag{6}$$

where Φ is the subspace composed of N global mode shapes, computed using just the elastic behavior of the viscoelastic material and considering multiple values of this modulus E_i (hence the name multi-model). The reduction basis T is then obtained by orthonormalization of the multiple modal bases.

To optimize the damping properties of the proposed joint design, damping of modes is computed for a range of complex moduli based on the above mentioned elastic modulus variation range, using the reduced model (5) as shown in Figure 6. This first computation is performed to assess the damping potential and thus uses a fixed loss factor $\eta=1$. It is noted that coupling computations would give similar results and understanding, but when a complex eigenvalue solver allows damping predictions these are the end objective and are thus preferred.

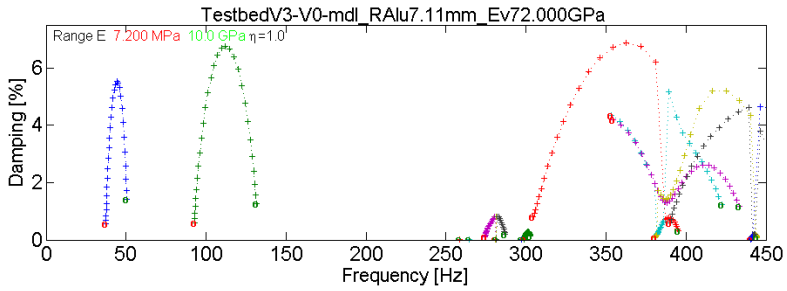

Figure 6 : Evolution of modal damping for a loss factor of $\eta=1$ and a viscoelastic modulus varying in the $[7.2\ MPa \quad 10\ GPa]$ range assuming total contact.

The mode shapes computed with the FEM model are shown in Figure 7. The first two modes are global bending. One then finds local modes of the upper panels, torsion and a second bending mode.

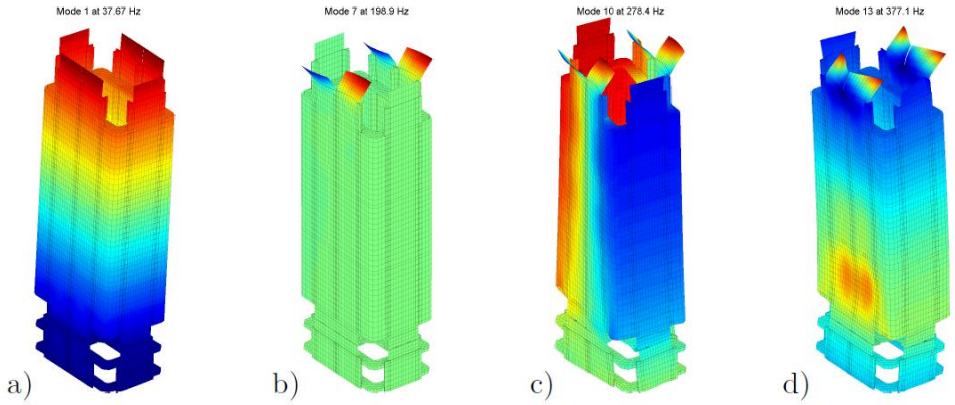

Figure 7 : FEM modes a) X bending (BendX), b) upper panel mode (SP_BX), c) torsion, d) second X bending (Bend2X)

The X bending near $50\,Hz$ has an optimal damping above 5%. The Y bending near $100\,Hz$ exceeds 6%. Near $250\,Hz$, a series of modes are almost not damped ($\xi < 0.5\%$). These are the modes of upper panels. Between $300\,Hz$ and $450\,Hz$, more highly damped modes correspond to modes of the web that significantly load the junction but being local modes are not very important in global dynamics. The torsion mode, below $300\,Hz$, and the second bending X mode just before $400\,Hz$, also exhibit some damping.

A different computation with a smaller surface of the metallic washer showed, as might be expected, an increase in damping. This shows that further work on the structuration of the contact surface would be useful.

While the initial study with fixed loss factor is useful to ascertain that significant modal damping can be achieved, true viscoelastic materials have simultaneous variation of modulus and loss factor and selection of the appropriate material is needed. For a given mode, one can thus generate a map showing the damping level as a function of modulus and loss factor. This is shown for the first mode of the testbed in Figure 8. The choice of presenting performance maps in this format is an originality of the software used here [6] and gives a simple understanding of the evolution of damping performance within the design space.

Finalizing a design implies choosing a viscoelastic material and its thickness. With that given, the actual modulus and loss factors as a function of temperature can be shown in the performance map. The generic trend is a decrease of modulus with temperature associated with a peak in loss factor at transition temperature. This evolution generates a bell shaped curve in the modulus and loss factor plane. In Figure 8, the evolutions of Smactane50 [24] and the harder Smactane70 are thus shown as dotted lines with text for each temperature point.

For the initial thickness of $1\,mm$, Smactane50 is too soft and good performance is only found for temperatures below -20°C. Smactane 70 seems more efficient from this point of view. The area density of viscoelastic layer tensile stiffness is given by

$$k = \frac{Ev}{h} \tag{7}$$

where stiffness is inversely proportional with thickness. Since the important parameter is stiffness and not modulus, one can increase stiffness, in other words shift the material law to the right in the performance map, by decreasing thickness.

This concept is illustrated in Figure 8 with the Smactane 50 of $1mm$ and $0.2\ mm$ of thickness. For the smaller thickness, a damping of 0.7% is reached for a temperature of 10°C. However, for $1mm$ of thickness, this value is reached for -10°C. The choice of the proper material will thus depend on availability in small thicknesses, temperature range of operation, durability, bonding process … but the performance map clearly illustrates that a mean rather than optimal performance should be selected.

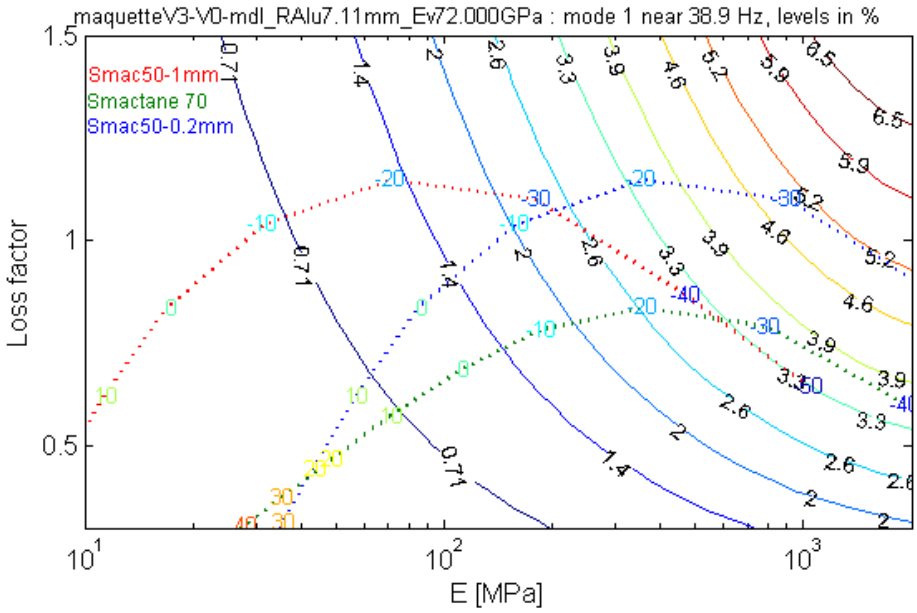

Figure 8 : Damping map of first bending mode in a space of Young's modulus and loss factor ranges with characteristics evolution of Smactane 50 (of $1mm$ and $0.2mm$ of thickness) and Smactane 70 (of $1mm$ of thickness) as a function of the temperature (dotted lines).

5. Experimental investigation

To validate the performance of the junction proposed in previous sections, an experimental modal test was carried out to allow test/analysis correlation. To study the variations of damping induced by the junction, three configurations are compared. A base bolting of the brackets with no viscoelastic treatment, called "dry contact", the addition of a $0.2mm$ thick layer of Smactane 50 ($E_v \in [50\ 70]MPa$, $\eta \in [0.48\ 0.7]$ for $[97.3\ 513.9]\ Hz$ at $25°C$) and the addition of a $1mm$ thick layer of Smactane 70 ($E_v \in [60\ 90]MPa$,$\eta \in [0.5\ 0.65]$ for $[97.3\ 513.9]\ Hz$ at $25°C$).

5.1 Modal test and damping performance

As shown in Figure 1, the small box was fixed to the ground, using small contact surfaces to minimize coupling. A hammer test at 80 points distributed over two perpendicular sides of the testbed was then used to measure modeshapes. Transfer functions were estimated from acceleration and force measurements. Modeshapes, frequencies and damping were then identified using a non-linear frequency domain output error method [25]. Figure 9 illustrates test bending modes which are very similar to the computed ones shown in Figure 7.

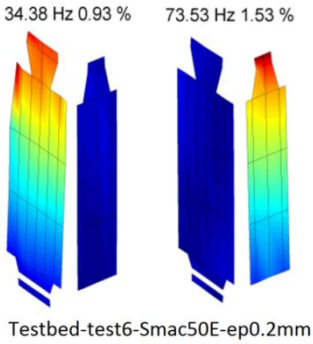

Figure 9 : Test derived X and Y bending modes

Measured transfer functions showed very different behavior in dry and viscoelastic junctions. Obtaining clean measurements was much harder for the dry configuration. The Nyquist plot near resonances, shown at Figure 10b, is clearly non-symmetric, which is an explicit indication of non-linearity [26]. For the damped configuration (Figure 10c), measurements were much easier and Nyquist plots indicate a much more linear behavior.

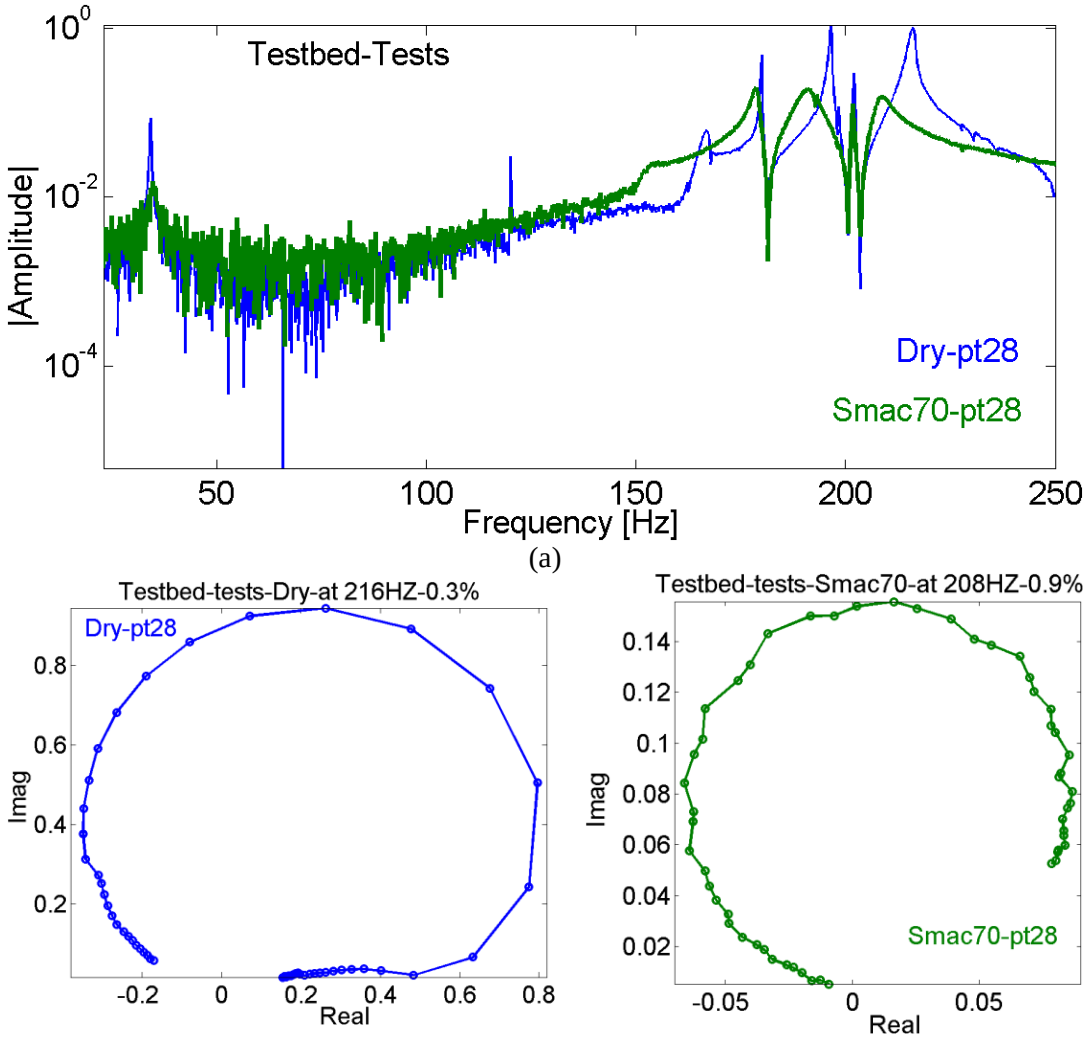

(a)

(b)

(c)

Figure 10: a) FRF signals for dry and with Smactane 70 configurations, b) Nyquist diagram for dry configuration at 216 Hz, c) Nyquist diagram for Smactane 70 configuration at 208Hz

The performance of the proposed design is demonstrated by the results shown in Figure 11. With Smactane 50/0.2 mm, the damping of global modes is increased by more than a factor 3. Local modes show a much smaller change, but this was predicted by the computations since the energy fraction present in the joint is very low for these modes. For the Smactane 70/1mm, the resulting stiffness is higher and as expected damping is higher (factor > 8). This is consistent with the results presented in section 4.

Including a compliant viscoelastic layer makes the structure somewhat more flexible. The frequency modifications illustrated in Figure 11b show that damping was achieved with minimal shifts in frequency, which in the present case are of the same order of magnitude as those associated with tolerances in the assembly process.

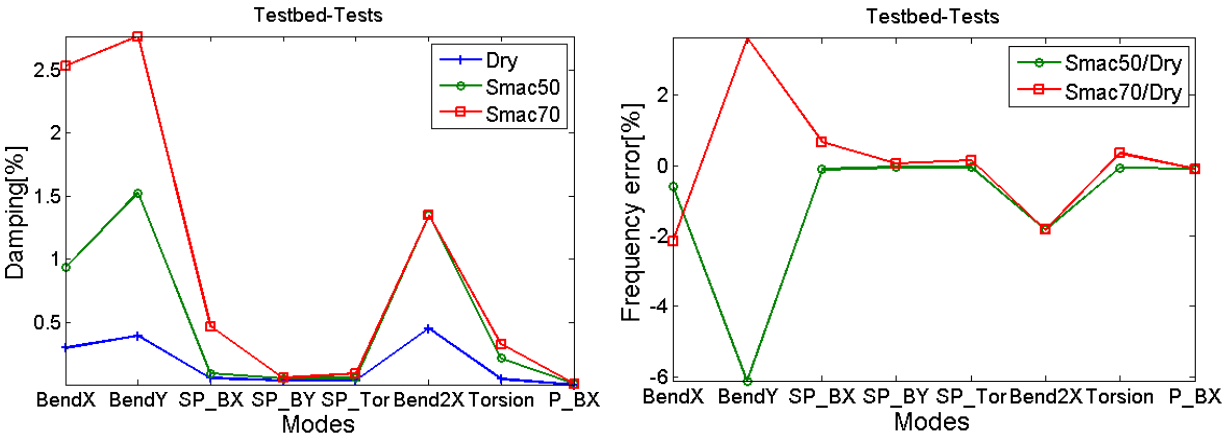

(a) (b)

Figure 11 : a) Evolution of damping with additional viscoelastic material, b) Evolution of frequency shift with additional viscoelastic material

It is clear that friction and non-linearity would increase the apparent damping in the dry configuration at sufficient excitation levels. Thus more classical sine or broadband excitation testing are necessary for a proper evaluation of damping induced by friction. Such damping however induces wear and does not operate well at low levels, hence the interest in alternative mechanisms such as viscoelasticity. It is worth noting that the tightening torque of 10 $N.m$ applied here was assumed sufficient to limit preload effects at low amplitudes, even though this was not further investigated.

5.2 Model updating

After dismantling to change configurations, prints were found on the viscoelastic layers (Figure 12b). These marks represent the real contact area obtained after tightening bolts to assemble the junction. The real contact area does not extend over the whole interface and this is due to geometrical defects of the testbed. Model adjustment was thus found to be necessary. A second model, called V2, uses partial bilateral contact on the red dots of Figure 12a, whereas the initial V0 assumed contact over the whole viscoelastic patch.

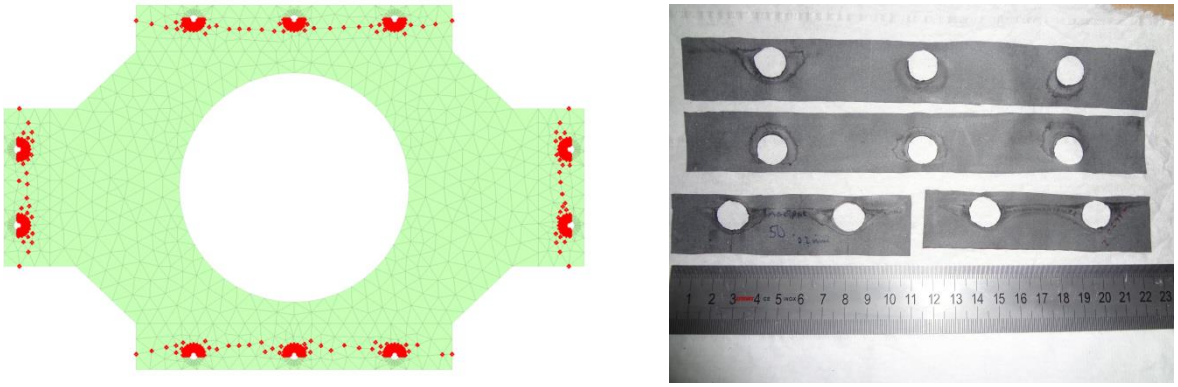

(a) (b)

Figure 12: a) Model of partial contact area, b) Viscoelastic layers after disassembly

Figure 13 clearly illustrates the improvement on predicted frequencies found with model V2.

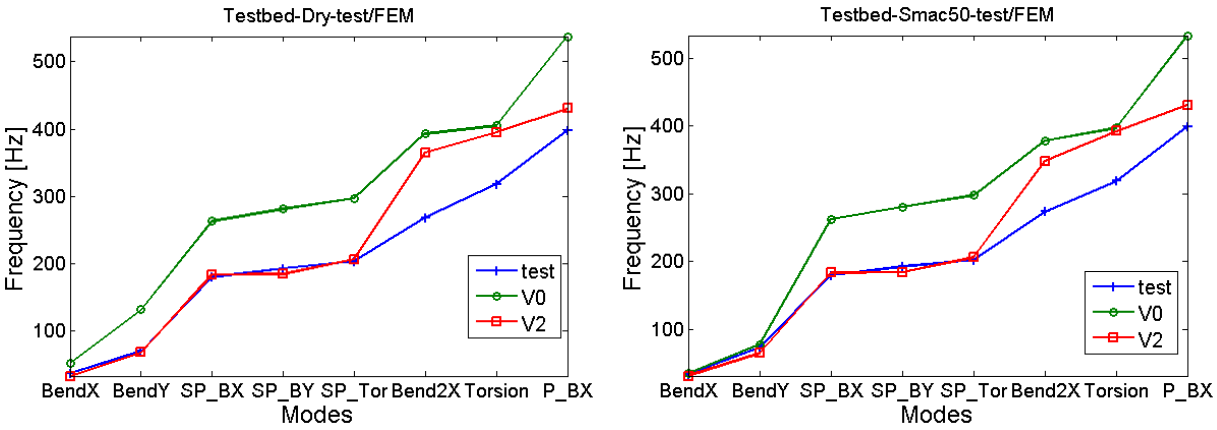

(a) (b)

Figure 13: Frequency evolution for the two versions V0 and V2 and the test data, a) for the Smactane 50 configuration, b) for the dry configuration

In terms of modeshapes, the MAC values shown in Figure 14 don't show significant sensitivity between test and numerical modes expect for the bend2X and the torsion mode. The first two bending modes in the Smactane 50 configuration represent 80% and 98% of MAC values when comparing experimental and numerical (respectively V0 and V2) results. Furthermore, updating model to version V2 enhances results in terms of frequencies (Figure 13). Taking a reduced contact area into account diminishes the numerical/experimental discrepancy from 49% to -4.8% for the first X Bending mode in the dry configuration for example. For upper panels modes (SP_BX, SP_BY and SP_T) frequencies are well adjusted with the V2 version for the dry and the Smactane 50 configurations. Likewise, for torsion mode, there is an over-estimation of the frequency which can be most likely attributed to welding modelling defects in the small box.

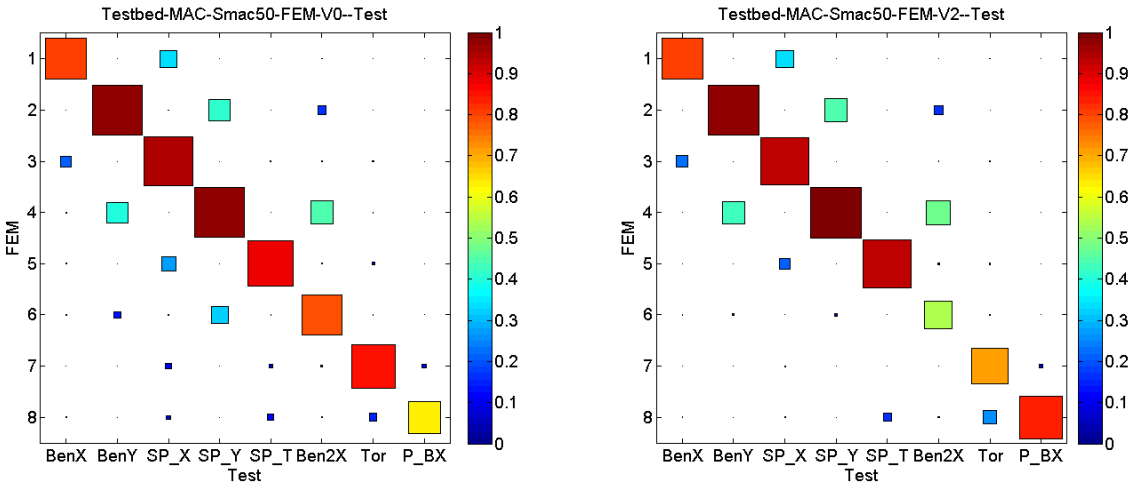

(a) (b)

Figure 14: MAC: computation/test correlation of the Smactane 50 configuration, a) with total contacts V0, b) with partial contact V2

The test/analysis correlation showing defects in the contact surfaces, the initial numerical design must be questioned. The search for optimal damping at fixed loss factor was shown in Figure 6 illustrated modal damping for model V0, the same result is shown in Figure 15 for model V2. The optimal damping decreases to less than 1% and 1.5% for the first two modes. A limitation of the proposed design is thus that junction design must ensure that proper contact is maintained. This result emphasizes the need for robust design.

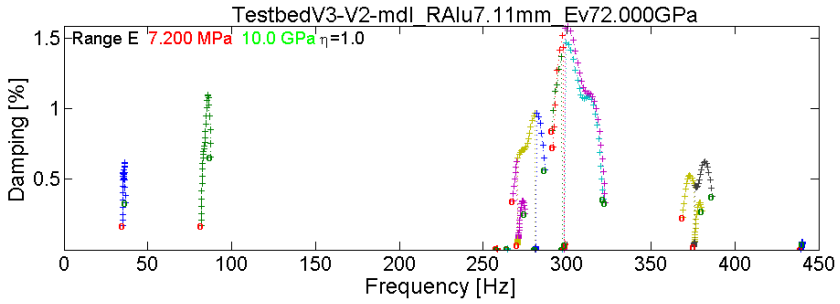

Figure 15 : Evolution of modal damping for a loss factor of η=1 and a viscoelastic modulus varying in the [7.2 MPa 10 GPa] range contact of model V2

6. Conclusion

The paper proposed a detailed case history on damping design of a jointed structure. Important notions that were illustrated are the level of junction coupling, which ensures that the junction has sufficient influence on the response to induce damping, the need to preserve static performance, and the ability to use numerical simulations and appropriate representations of the performance/design space to find optimal or robust damping behavior. The experimental realization featured performance with damping increase by a factor 3 to 8 depending on the design. This improvement is consistent with the numerical predictions, but the test also showed the importance that geometric defects can have. Processes with polymerization on the assembled structure seem a possible strategy to address the problem. The proposed structuration of the contact surface is a first attempt at introducing viscoelastic damping in

bolted junctions. Geometric optimization can clearly be achieved numerically and seems an interesting perspective for future work. Integrating robustness to temperature, geometric defects, aging, etc. in a design process with both static and dynamic objectives seems another major challenge for which models will play a key role.

7. Acknowledgements

This work was part of the FUI/MAIAS project on the “mastering of damping in junctions” labeled by pole ASTECH.

References

[1] C. F. Beards and J. L. Williams, “The damping of structural vibration by rotational slip in joints,” J. Sound Vib., vol. 53, no. 3, pp. 333–340, Aug. 1977.
[2] C. F. Beards and A. Woowat, “The control of frame vibration by friction damping in joints,” J. Vib. Acoust. Stress Reliab. Des., vol. 107, no. 1, pp. 26–32, 1985.
[3] R. P. Donnelly Jr and R. L. Hinrichsen, “The effect of energy dissipation due to friction at the joint of a simple beam structure,” Math. Comput. Model., vol. 11, pp. 1022–1027, 1988.
[4] R. Wang, A. Crocombe, G. Richardson, and C. Underwood, “Modelling of damping in small satellite structures incorportaing bolted joints,” in 19th Annual AIAA/USU, Small Satellite Conference, 2005.
[5] E. Balmes and Germès, S., “Tools for Viscoelastic Damping Treatment Design. Application to an Automotive Floor Panel,” in Int. Seminar on Modal Analysis, Leuven, 2002.
[6] E. Balmes and al., “Viscoelastic vibration toolbox, User’s guide” SDTools , Jul. 2007 www.sdtools.com/pdf/visc.pdf.
[7] L. Heller, “Amortissement dans les structures assemblées,” PHD thesis, UFR des sciences et techniques de l’université de Franche-Comté, 2005.
[8] L. Gaul, S. Hurlebaus, J. Wirnitzer, and H. Albrecht, “Enhanced damping of lightweight structures by semi-active joints,” Acta Mech., vol. 195, no. 1–4, pp. 249–261, 2008.
[9] L. Gaul and J. Lenz, “Nonlinear dynamics of structures assembled by bolted joints,” Acta Mech., vol. 125, no. 1–4, pp. 169–181, 1997.
[10] J. Abad, J. M. Franco, R. Celorrio, and L. Lezàun, “Design of experiments and energy dissipation analysis for a contact mechanics 3D model of frictional bolted lap joints,” Adv. Eng. Softw., vol. 45, no. 1, pp. 42–53, 2012.
[11] S. Le Loch, “Modélisation et identification de l’amortissement dans les structures spatiales,” PHD thesis, Ecole normale supérieure de Cachan, 2003.
[12] A. Caignot, P. Ladevèze, D. Néron, and J.-F. Durand, “Virtual testing for the prediction of damping in joints,” Eng. Comput. Swans. Wales, vol. 27, no. 5, pp. 621–644, 2010.
[13] L. Heller, E. Foltête, and J. Piranda, “Damping identification of assembled structures,” Mec. Ind., vol. 7, no. 4, pp. 351–363, 2006.
[14] A. D. Crocombe, R. Wang, G. Richardson, and C. I. Underwood, “Estimating the energy dissipated in a bolted spacecraft at resonance,” Comput. Struct., vol. 84, no. 5–6, pp. 340–350, 2006.
[15] L. Roger, C. Johnson, and D. Keinholz, “The modal strain energy finite element method and its application to damped laminated beams,” Shock Vib. Bull., vol. 51, 1981.
[16] N. W. Hagood, W. H. Chung, and A. V. Flotow, “Modelling of Piezoelectric Actuator Dynamics for Active Structural Control,” J. Intell. Mater. Syst. Struct., vol. 1, no. 3, pp. 327–354, Jul. 1990.
[17] R. Kellermann and H. C. Klein, “Untersuchungen über den Einfluß der Reibung auf Vorspannung und Anzugsmoment von Schraubenverbindungen,” Konstruction Springer Verl., vol. 2, 1955.
[18] J. Kim, J.-C. Yoon, and B.-S. Kang, “Finite element analysis and modeling of structure with bolted joints,” Appl. Math. Model., vol. 31, no. 5, pp. 895–911, 2007.
[19] J. Montgomery, “Methods for modeling bolts in the bolted joint,” in ANSYS User’s Conference, 2002.
[20] J. Rasmussen, I. B. Norgaard, O. Haastrup, and J. Haasturp, “A two body contact problem with friction,” in Euromech Colloquim NR 110 Rimforsa, 1978, pp. 115–120.

[21] C. Hammami, “Intégration de modèles de jonctions dissipatives dans la conception vibratoire de structures amorties,” PHD thesis, École Nationale Supérieure d’Arts et Métiers, Paris, 2014.
[22] Franck Renaud, Jean Luc Dion, Gael Chevallier, Imad Tawq, Remi Lemaire. A new identication method of viscoelastic behavior : Application to the generalized Maxwell model. Mechanical Systems and Signal Processing, Elsevier, 2011, 25, pp.991-1010.
[23] E. Balmes, “Parametric families of reduced finite element models. Theory and applications,” Mech. Syst. Signal Process., vol. 10, no. 4, pp. 381–394, 1996.
[24] T. Demerville and P. Bastia, “Original Elastomeric Dampers for the EXPERT Reentry Vehicle,” in ESA ESMATS, Germany, 2011.
[25] E. Balmes, “Frequency domain identification of structural dynamics using the pole/residue parametrization,” presented at the International Modal Analysis Conference, 1996, pp. 540–546.
[26] J. Piranda, “Analyse modale expérimentale,” vol. base documentaire : TIB420DUO, 2001.